Chem Soc Rev

Point-of-care biochemical assays using gold nanoparticle-implemented microfluidics

Journal:	*Chemical Society Reviews*
Manuscript ID:	CS-TRV-04-2014-000125.R1
Article Type:	Tutorial Review
Date Submitted by the Author:	18-May-2014
Complete List of Authors:	Sun, Jiashu; National Center for Nanoscience and Technology, Xianyu, Yunlei; National Center for Nanoscience and Technology, Jiang, Xingyu; National Center for Nanoscience and Technology,

Point-of-care biochemical assays using gold nanoparticle-implemented microfluidics

Jiashu Sun[a], Yunlei Xianyu[a] and Xingyu Jiang[*a]

[a] *Beijing Engineering Research Center for BioNanotechnology & Key Lab for Biological Effects of Nanomaterials and Nanosafety, National Center for NanoScience and Technology, Beijing, P. R. China, 100190*

E-mail: xingyujiang@nanoctr.cn;

Abstract

One of the goals of point-of-care (POC) is a chip-based, miniaturized, portable, self-containing system that allows the assay of proteins, nucleic acids, and cells in complex samples. The integration of nanomaterials and microfluidics can help achieve this goal. This tutorial review outlines the mechanism of assaying biomarkers by gold nanoparticles (AuNPs), and the implementation of AuNPs for microfluidic POC devices. In line with this, we discuss some recent advances in AuNPs-coupled microfluidic sensors with enhanced performance. Portable and automated instruments for device operation and signal readout are also included for practical applications of these AuNPs-combined microfluidic chips.

Key learning points

(1) Mechanism of assaying biomarkers by gold nanoparticles (AuNPs).

(2) Design and realization of microfluidic tools for POC assays.

(3) Development of new POC tools based on AuNPs-coupled microfluidics.

(4) Development of portable and automated instruments for POC devices.

1. Introduction

The development of point-of-care (POC) biochemical assays has provided promising tools for rapid and routine diagnosis and assessment of diseases. If affordable POC diagnostics is developed, underdeveloped regions that previously have no access to advanced diagnostic tools can benefit, while patient care in developed countries can also be improved. The most common types of detection of biomarkers include proteins, nucleic acids, other biomolecules and cells, which are found in complex bodily fluids such as blood and urine. One of the goals of POC testing is to come up with a chip-centered, miniaturized, portable, self-containing system that allows the assay of biomarkers of complex samples. To achieve this goal, some prerequisites should be acknowledged for developing POC assays: 1) The chip has to be small and easy to operate; 2) The instrument has to be portable and automated; 3) The entire process of the assay from pretreatment of sample to readout of data requires no human interference. This goal has only been partially realized.[1] For instance, lateral flow assays (LFA) can accommodate complex samples such as whole blood and yield results for protein biomarkers and some small molecules, but LFA is limited in assaying for nucleic acids.

Microfluidic technology is an enabling technology for POC tests because it allows reduced sample/reagent consumption, integrated components and functions, and high portability and flexibility. Although many microfluidics-based diagnostic prototypes have been well demonstrated by the academic community, few of them are commercially launched in the market due to several challenges. One major challenge is that an easy-to-operate chip that carries out an assay inevitably requires complicated fluid circuits and even microfabricated valves or pumps. To precisely handle minute amounts of fluids and actuate

valves or pumps, expensive and large external equipments are often necessary. Another challenge is the lack of miniaturized detection/readout system for real-time measurement. An ideal readout for microfluidic assays should be portable, rapid, sensitive and quantitative, while supporting a wide dynamic range of detection.

Gold nanoparticles (AuNPs) have been widely adopted for the detection of ions/small molecules, nucleic acids (including DNA and RNA), and proteins. Typically, AuNPs include gold nanospheres, hollow spheres, nanorods and nanorings with varying optical/electrical properties. Several features of AuNPs suggest that they would be ideal for POC assays: good stability, visible color change upon aggregation, easily functionalized with biomolecules, and remarkable enhancement of signal in nanoscale geometries. Latest innovations of AuNPs-based diagnostics include improving the sensitivity and specificity of assays, and expanding their range of targets. The combination of AuNPs and microfluidics may ultimately pave the road to efficient strategies with enhanced performance and reduced complexity, which can be transferred into simple and cost-effective POC tests with minimal equipment, allowing untrained personnel to detect multiple biomarkers in real samples.

This tutorial review introduces four strategies: colorimetric/optical sensing, electrochemical sensing, surface plasmon resonance (SPR), and surface-enhanced Raman scattering (SERS), based on the use of AuNPs for detecting proteins and nucleic acids. These sensing schemes are involved for designing AuNPs-coupled microfluidic chips for POC biochemical assays. The requirement of portable and automated instrument customized for these chips is further discussed. For the types of biological markers and related diseases that utilize these technologies, Table 1 provides easy access. Each figure is accompanied by

a line of text that briefly explains the technology. In line with guidelines for Tutorial Reviews, only the most relevant references have been selected as examples.

2. AuNPs-based colorimetric assays

Colorimetric detection of biomarkers is of great importance for practical POC applications due to its straightforward operation and convenient readout. One of the most widely used nanomaterials for the construction of colorimetric sensors is AuNPs. AuNPs can be functionalized with sensing probes such as antibodies and nucleic acids, as well as chemical ligands to trigger the assemblies of AuNPs.[2] The aggregation of AuNPs (normally 10 – 50 nm in diameter) results in a visible color change of solution from red to blue, because of the inter-particle plasmon coupling.[3] This color change provides a practical means of designing colorimetric sensors for a variety of target analytes. Comprehensive reviews are available on colorimetric detection of proteins and nucleic acids using AuNPs,[4] and herein we only highlight a few examples with improved sensitivity and simplified operation that may be potentially applied for POC applications.

2.1 Colorimetric assays for proteins and some small molecules

Immunoassay is one of the most powerful clinical tools for protein assays, relying on the specific affinities between the antibody and the antigen to assay either the antigen or the antibody. The current strategies for immunoassays employ enzyme-labeled or fluorescent secondary antibodies, typically needing bulk instruments and/or skilled personnel for readout. This limitation is a challenge for adopting immunoassays into POC formats.

Our group reported a convenient but effective AuNPs-based immunoassay by using

copper monoxide nanoparticle (CuO NP)-labeled antibody as the secondary antibody that enabled the ultrasensitive detection of analytes with the naked eye.[5] To apply this assay for HIV diagnosis, the HIV-1 gp41 antigen was first incubated and blocked in the well plate, and serum sample containing anti-gp41 IgG was added to the same well, followed by secondary antibody labeled with CuO NPs. After immunoreaction, Cu^{2+} was released into the solution by hydrochloric acid, and the detection mixture composed of azide- and alkyne-modified AuNPs and sodium ascorbate was added. The aggregation of functionalized AuNPs occurred as a result of click chemistry in which copper acted as a catalyst, giving rise to the solution color change from red to blue (Fig. 1a). In this AuNPs-assisted colorimetric immunoassay, the limit of detection (LOD) of anti-gp41 IgG by the naked eye was about 150 ng/mL, which surprisingly, was at the same level as that measured by UV-Vis spectroscopy, and comparable to commonly used absorbance or fluorescence readout systems. This assay was also highly specific even in the presence of high concentrations of mixtures of other interfering molecules, and thus could be used for real patient samples (including complex mixtures such as serum).

Quantifying total protein concentration could also be achieved in a similar way using the click chemistry. As the catalyst for click reaction, Cu^{+} ensured both the sensitivity and selectivity of the assay. Proteins and peptides could help reduce Cu^{2+} to Cu^{+} depending on the number of peptides bonds, thus triggering the coupling of azide- and alkyne-modified AuNPs, and resulted in the aggregation leading to a color change of AuNPs (Fig. 1b). The number of peptide bonds is directly related to the total amount of peptides and proteins. This total protein assay had a wide detection range from 30 to 2500 μg/mL and could be applied for the quantitative determination of proteins in complex samples.[6]

In addition to being employed for visual readout, AuNPs could serve as fluorescence quenchers. Close proximity to AuNPs would result in the fluorescence quenching of fluorescent dyes. Based on this principle, we developed a dual-readout (both colorimetric and fluorometric) assay for acetylcholinesterase (AChE) using Rhodamine B-modified AuNPs (RB-AuNPs) (Fig. 1c).[7] Positively charged thiocholine, which was generated by the AChE-catalyzed hydrolysis of acetylthiocholine (working as the substrate), induced the aggregation of AuNPs due to the electrostatic interaction. This dispersion-to-aggregation process enabled colorimetric detection of 1 mU/mL AChE. Meanwhile, the generated thiocholine replaced the RB (originally fluorescence-quenched) from AuNPs due to the Au-thiol interaction, thus leading to a fluorescence recovery. In this way, the LOD could be achieved down to 0.1 mU/mL. Because fluorescence readout invariably requires much more complex equipments than color-change based assays, we have not included too many of these examples in this review. The principle of all these cases is based on the target-induced aggregation of AuNPs to present a red-to-blue color change.

Other colorimetric sensing strategies have been exploited by utilizing the property of large surface-to-volume ratio of non-spherical AuNPs such as gold nanorods (AuNRs). We reported a colorimetric glucose assay based on negatively charged AuNRs-enhanced generation of silver nanoparticles (AgNPs) (Fig. 1d).[8] Due to the electrostatic effect and large surface-to-volume ratio, AuNRs could efficiently enrich silver ions, and thus enhance the redox reaction with glucose on the surface of AuNRs. At the nanoscale, the generated AgNPs enabled a visible and straightforward readout. A working range from 0.07 μM to 4 μM could be achieved for quantitative analysis of glucose in human plasma samples.

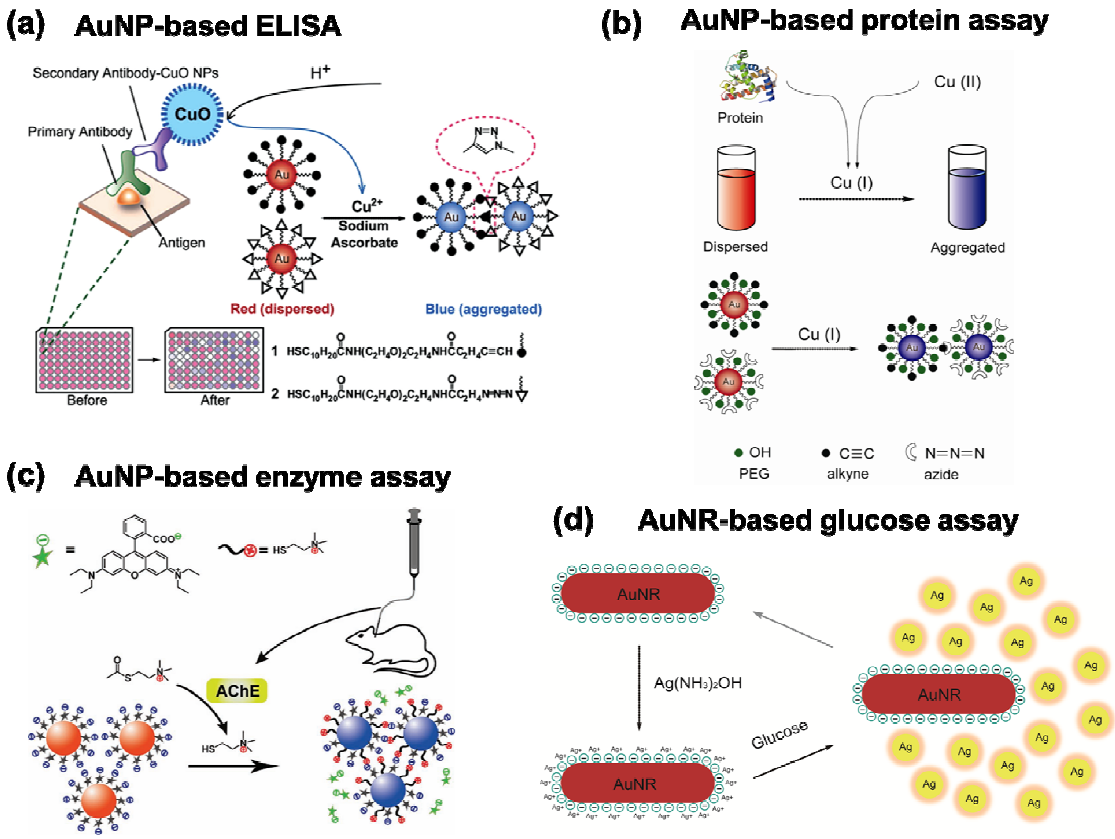

Fig. 1 Schematics of colorimetric immunoassay for protein detection using CuO-labeled secondary antibody. The functionalized AuNPs undergo aggregation as a result of click chemistry in which copper acts as a catalyst, giving rise to the solution color change from red to blue. Reprinted with permission from ref. [5], Copyright 2011 Wiley-VCH. (b) A colorimetric protein assay using click chemistry. Protein acts as a reducing agent to generate Cu^{+}, leading to the aggregation of azide- and alkyne-modified AuNPs. Reprinted with permission from ref. [6], Copyright 2012 American Chemical Society. (c) A dual-readout (colorimetric and fluorometric) assay of AChE using RB-AuNPs. Thiocholine derived from the catalysis of AChE lead to the aggregation of RB-AuNPs as well as the fluorescence recovery of RB. Reprinted with permission from ref. [7], Copyright 2012 Wiley-VCH. (d) A colorimetric glucose assay based on AuNRs-enhanced generation of AgNPs. Negatively

charged AuNRs enrich silver ions to enhance the redox reaction with glucose. Reprinted with permission from ref. [8], Copyright 2013 Royal Society of Chemistry.

2. 2 Colorimetric assays for nucleic acids

Nucleic acids (including DNA and RNA) are crucial for organisms due to their indispensable roles in encoding and expressing genetic information. Detection of nucleic acids provides considerable information for genetic diseases, pathogen infections and the diagnosis/treatment of cancers. Conventionally, techniques like polymerase chain reaction (PCR) are widely implemented for the identification of nucleic acids in research and clinical practice. Though performing well in both accuracy and sensitivity, the requirement for tedious procedures and specialized instruments presents a challenge for on-site detection for nucleic acids, which requires the convenient and straightforward readout. Mirkin *et al.* pioneered studies on the DNA-meditated assembly of AuNPs, making possible the colorimetric assays for detection of nucleic acids (Fig. 2a).[9] Thiolated DNA strand could assemble on the surface of AuNPs through Au-thiol interactions. The base sequences of thiolated DNA were designed to make complementary ends to the target DNA. The introduction of target DNA altered the inter-particle distance via DNA base-pairing (hybridization), thus affecting the distance-dependent optical properties of AuNPs. Due to the hybridization feature of DNA and the high extinction coefficient of AuNPs, 10 fmol of nucleic acids could be detected with naked eyes.

Apart from functionalized AuNPs, unmodified AuNPs have been utilized for colorimetric detection of nucleic acids as well. Li *et al.* reported the different behaviors of

single-stranded and double-stranded DNA (ssDNA and dsDNA) absorbed on unmodified AuNPs (Fig. 2b).[10] Owing to the electrostatic repulsion between negatively charged phosphate backbone of dsDNA and citrate-capped AuNPs, it would prevent dsDNA from absorption on AuNPs. The addition of salt would eliminate this repulsive interaction, leading to the aggregation of AuNPs. However, ssDNA could bind on the surface of AuNPs due to the high affinity between its bases and AuNPs. Even a high concentration of salt would not induce the aggregation of AuNPs due to lack of electrostatic interaction. Based on the difference in the electrostatic properties of ssDNA and dsDNA, a simple colorimetric hybridization assay was designed. A small amount of 4.3 nM nucleic acids could be visually detected with the single-base mismatches.

Compared with functionalized AuNPs, the utilization of unmodified AuNPs circumvents the drawbacks (like limitations of specific ligands and complicated labeling procedures) and shows superiority in POC detection due to its simplicity and convenience.[11] Recently, Xia *et al.* developed a versatile sensor for colorimetric detections of multiple analytes including nucleic acids, proteins, small molecules and metal ions (Fig. 2c).[12] The principle of this approach relies on the preferential binding capabilities of cationic water-soluble conjugated polymers with ssDNA over dsDNA. In this work, they found that both of these two types of DNA could stabilize the unmodified AuNPs in diluted salt solution. However, because of the higher affinity of ssDNA with conjugated polymers than dsDNA, the binding between target DNA and ssDNA would deprive ssDNA from AuNPs to result in the aggregation of AuNPs accompanied with a remarkable color change of the solution. A sensitivity of 1.25 pM target DNA could be achieved by the naked eye. Other target species (like proteins, organic molecules and

inorganic ions) could be indirectly detected as well by employing aptamers (functional nucleic acids that can specifically bind with high affinity to targets) into this system.

Another important approach for the optical nucleic acid assay is "gold label silver stain" (GLSS). In the GLSS process, AuNPs act as the catalyst to promote the reduction of silver ion to form silver shells around AuNPs for signal enhancement. This approach can reach a considerably high sensitivity. The generated silver shells can be visualized with naked eyes. GLSS is typically carried out on a solid substrate and target nucleic acids can be identified directly in an instrumentation-free manner. This technique provides an excellent opportunity to develop POC assays for medical diagnostics.

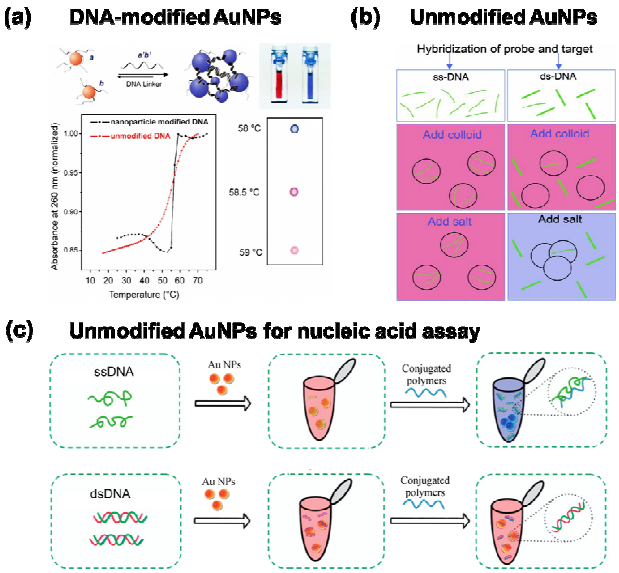

Fig. 2 Colorimetric assays for nucleic acid detection. (a) Hybridization of target DNA with complementary probe DNA modified on AuNPs, leading to the aggregation accompanied with a color change from red to blue. Reprinted with permission from ref. [9], Copyright 2006 Elsevier. (b) Unmodified AuNPs for DNA analysis based on the different absorption behaviors of ssDNA and dsDNA. Reprinted with permission from ref. [10],

Copyright 2004 National Academy of Sciences. (c) Conjugated polymers-modified AuNPs as a versatile sensor for multiple analytes. Binding events induce the deprivation of ssDNA from AuNPs, resulting in the aggregation with a remarkable color change of the solution. Reprinted with permission from ref. [12], Copyright 2010 National Academy of Sciences.

2.3 AuNPs-based lateral flow assays (LFA) for proteins

LFA has played a dominant role in POC diagnostics which allows the one-step, rapid and instrumentation-free analysis of proteins in complex samples. Commercial lateral flow strips mainly rely on labeled AuNPs for optical detection, and have been widely applied for testing pregnancy, HIV, influenza, and biological analytes.[13, 14] Typically, a lateral flow strip consists of a sample pad, a conjugate pad, a reaction membrane, and an absorbent pad (Fig. 3a).[15] All these components are assembled on a plastic adhesive backing layer or enclosed in a plastic cassette. The sample pad is made of porous materials such as cellulose fiber, to evenly distribute the sample, or/and providing a filter structure for sample pretreatment. The treated sample migrates toward the conjugate pad by capillary action and interacts with the antibody-conjugated AuNPs (for sandwich immunoassays). The formed complex further moves toward the reaction membrane, in which two lines of antibodies (a test line and a control line) are immobilized. After the immunoreaction, a red color appears at the test line in the presence of the target analyte, caused by the accumulation of captured AuNPs. The control line also becomes red to confirm the sample wicking through the absorbent pad. The result of LFA can be directly observed with the naked eye.

As an alternative to antibody, aptamer was also adopted to label AuNPs for preparing the conjugation pad of lateral strip. Aptamers are easy to produce, high in binding affinity to target proteins, and compatible to AuNPs. Xu *et al.* designed and fabricated aptamer-functionalized AuNPs as the conjugate probes, instead of antibody-labeled AuNPs, for detecting thrombin in human plasma samples by LFA.[16] After thrombin solution was added into the sample pad, the binding between rehydrated aptamer-labeled AuNPs and thrombin occurred at the conjugate pad to form the thrombin-aptamer-AuNPs complex (Fig. 3a). This complex was captured by another aptamer immobilized on the test line of the reaction membrane, indicated by a characteristic red band. The control line also exhibited a red color due to the hybridization between the excess labeled AuNPs and controlled probes. The LOD of this aptamers- and AuNPs-based immunoassay was 0.6 pmol for thrombin in human plasma. Apart from the direct readout of results by the naked eye, the quantitative detection could be realized by using a portable strip reader.

Despite of these tremendous advantages of LFA for practical applications, the sensitivity of AuNPs-based LFA is lower than that of immunoassays with fluorescent or enzyme-colorimetric readout. To improve the sensitivity of LFA without scarifying its simplicity, Choi and co-workers utilized two kinds of antibody-labeled AuNPs with different sizes to construct the conjugate pad.[17] The first AuNPs of 10 nm were combined with the analyte through antibody-antigen interaction, and the second AuNPs of a larger size (40 nm) subsequently bound with the first AuNPs, and amplified the signal of test line by 100 times (Fig. 3b). This dual AuNP conjugate-based LFA could detect troponin I as low as 0.01 ng/mL, and be used for assaying the serum samples of patients with

myocardial infarction. Another signal-amplification strategy for lateral flow immunoassays was based on the use of AuNPs as the labeling carriers for horseradish peroxidase (HRP)- modified antibodies. The analyte solution was first dispensed onto the sample pad to initiate the reaction. After washing off the excess antibody-labeled AuNPs, the lateral strip was dipped into the HRP substrate to produce a dark color band at the test line, which was quantified by a strip reader. Although this method could increase the detection sensitivity up to one order of magnitude, it involved several washing steps and additional solutions. Another approach for enhancing the sensitivity of lateral flow immunoassays was to extend the conventional lateral strip to the two-dimensional paper network, in which multiple rinse and signal amplification steps were intergrated.[18, 19]

2.4 AuNPs-based colorimetric assays for nucleic acid detection

2.4.1 AuNPs-based LFA for nucleic acids

Because using LFA to detect proteins (and some small molecules) has become fairly successful, researchers have recently attempted to assay nucleic acids using LFA. The current LFA for testing nucleic acids can be subdivided into two major types: direct detection of nucleic acids without amplification, and detection of amplified products of nucleic acid using PCR or isothermal amplification (unlike PCR that requires cycling through different temperatures, isothermal amplification takes place at a constant temperature). The LFA for DNA detection without amplification was demonstrated by Mao *et al.* by using a sandwich DNA hybridization reaction.[20] The sample solution with target DNA was first hybridized with DNA-AuNP probes at the conjugate pad. The formed complex continued to flow through the test line in which the second hybridization

occurred between the target DNA and the immobilized DNA probes, appearing as a red band. At the control line, a second red line was visualized due to the hybridization between excess DNA-labeled-AuNPs and the other DNA probes. This nucleic acid LFA could detect the target DNA in the range of 1-100 nM in less than 15 min, without extra incubation, mixing, and washing steps.

To enhance the sensitivity and the specificity of nucleic acid detection, a pre-amplification step for target DNA/RNA is commonly adopted by using PCR or isothermal amplification. The LFA is then used as a detection method for amplified product, which may increase the sensitivity over six orders of magnitude as compared to direct detection of nucleic acids by LFA. Lie and co-workers reported a LFA for detecting amplified DNA by isothermal strand-displacement polymerase reaction (Fig. 3c).[21] The target DNA was first conjugated to the hairpin-DNA-probe-modified AuNPs, and the amplified DNA-AuNP complex was captured by another DNA probe immobilized on the test line via hybridization. This system allowed for the detection of target DNA as low as 0.01 fM within 30 min by the naked eye, and the LOD of human genome DNA was around 25 ng/mL.

2.4.2 Microfluidic-based LFA for nucleic acids

A sensitive POC LFA for nucleic acids should integrate DNA/RNA amplification, which generally requires bulky instruments, expensive reagents, and trained technicians. The conventional architecture of lateral stripe cannot realize this complicated procedure. To overcome this limit, Nagatani *et al.* designed a microfluidic continuous-flow reverse transcription-PCR (RT-PCR) chip to amplify influenza virus RNA using a FITC-labeled

primer and the biotinylated primer.[22] The amplified product was mixed with biotin antibody-labeled AuNPs to form the complex, and detected by the immobilized FITC antibody at the test zone. The total assay time including RNA amplification and LFA detection was less than 30 min, and the LOD was 4 pg/μL by the naked eye. An additional advantage of this system is that the confinement of reaction mixtures in microfluidic channels avoids the degradation of RNA. A small, proof-of-concept lateral chip made of plastic and paper was demonstrated to perform an isothermal amplification of HIV DNA, the product of which was detected by another LFA.[23] The amplification time for 10 copies of HIV DNA to detectable levels was less than 15 min. In the above sensing schemes, the nucleic acid amplification and LFA detection are still separated.

Kim *et al.* proposed a fully integrated microfluidic system composed of a RT-PCR reactor for viral RNA amplification, and a lateral strip for colorimetric detection (Fig. 3d).[24] In the RT-PCR chamber, the target sequences from H1N1 viral RNA was amplified by the Texas Red-labeled primer and biotin-dUTP. The RT-PCR product was transferred to the conjugate pad of the lateral strip, and linked with functionalized AuNPs by actuating the on-chip pneumatic pump. The conjugations were captured by streptavidin on the test line to appear as a red line, and the excess labeled AuNPs reacted with the anti-mouse IgG at the control line. The total assay time was within 2.5 hr, and the LOD was 14.1 pg of RNA templates. Moreover, a customized, and portable instrument for controlling the microfluidic device and analyzing the LFA result was developed to provide an advanced platform for POC diagnostics.

Today, the most successful commercial product using AuNPs for practical POC applications is the lateral strip for protein detection, with its important features of simple

operation and rapid/visible readout. To quantify the detection result, the small and portable strip reader was designed. In comparison, the application of lateral strip for POC nucleic acid analysis still needs some improvements including the integration of DNA/RNA pretreatment, the buffer storage into the device, and the simplification of operation and readout.

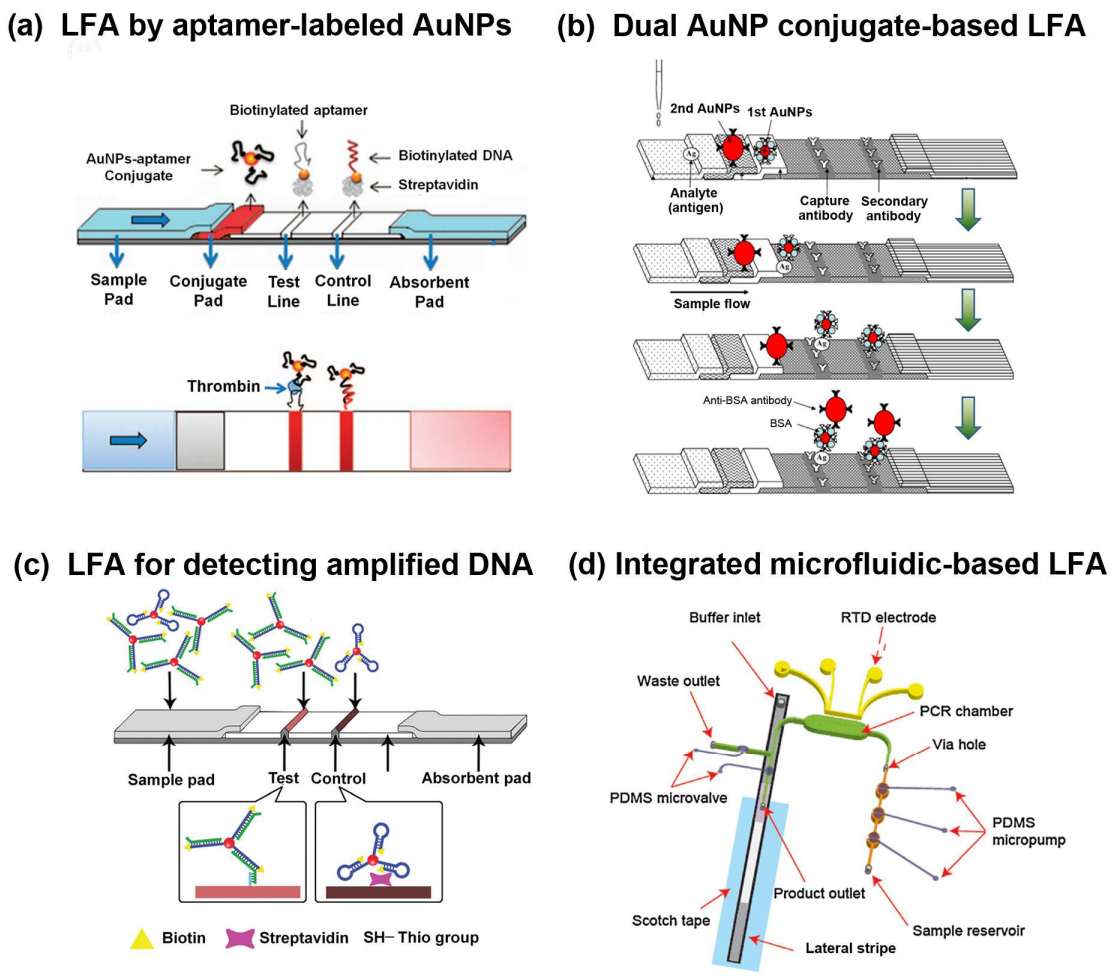

Fig. 3 (a) LFA using aptamer-functionalized AuNPs as the conjugate probes for detecting thrombin in human plasma samples. Reprinted with permission from ref. [16], Copyright 2009 American Chemical Society. (b) The dual AuNP conjugate-based LFA for assaying

troponin I with enhanced sensitivity. Reprinted with permission from ref. [17], copyright 2010 Elsevier. (c) The LFA for detecting amplified DNA by isothermal amplification. Reprinted with permission from ref. [21], copyright 2012 Royal Society of Chemistry. (d) Schematics of an integrated microfluidic system composed of a RT-PCR reactor for viral RNA amplification, and a lateral strip for colorimetric detection. Reprinted with permission from ref. [24], copyright 2012 Elsevier.

3. AuNP-based electrochemical assays

The unique properties of AuNPs, including excellent conductivity, good catalytic activity, and high surface-to-volume ratio have provided considerable promise for designing electrochemical sensors over a wide range of biomarkers.[25] To construct an electrochemical biosensor, some researchers use AuNPs to modify the working electrodes, enabling direct electron transfer from redox-active protein to the electrode surface. Meanwhile, AuNPs could also serve as carriers for biomarker probes or electroactive labels. Some studies also employ AuNPs for enhancing the efficiency of electrochemical sensing. Compared with AuNPs-based optical detection, electrochemical assays could be easily multiplexed using an electrode array without relying on bulky components, which are perfectly suited to POC diagnostics.

3.1 AuNPs-based microfluidic electrochemical immunoassay

Microfluidics can effectively downscale the conventional AuNPs-based electrochemical assays into POC formats, while keeping their inherent advantages. Chen and co-workers reported a microfluidic electrochemical immunoassay to detect hemoglobin A1c (HbA1c,

a biomarker for diabetic patients) by using nanoparticles (NPs), composed of the gold outer shell, chitosan middle shell, and Fe_3O_4 core (Fig. 4a).[26] Before electrochemical immunoassay, the outer gold layer of NPs was coated with HbA1c antibody. The immobilization of labeled NPs inside the detection region of microfluidic channel was realized by an external magnetic field. After the on-chip electrokinetic injection and electrophoretic separation of HbA1c from blood samples, HbA1c was conjugated to antibody-coated NPs via the sandwich immunoassay. A subsequent electrochemical reaction was performed after immunoassay, and the concentration of captured HbA1c was proportional to the current change. This microfluidic electrochemical immunoassay system could detect HbA1c from a complex sample within 30 min, and the response of HbA1c was linear in the range of 0.05 - 1.5 μg/mL. Chikkaveeraiah *et al.* developed another microfluidic electrochemical immunoassay system for ultra-sensitive detection of two protein cancer biomarkers (prostate specific antigen, PSA, and interleukin-6) in serum at sub-pg/mL levels.[27] This system featured the deposition of glutathione-modified AuNPs onto the electrode surface, providing the biocompatible surface and the increased area for binding capture antibodies. The cost of each microfluidic chip for simultaneous detection of 4 proteins was approximately 10 dollars.

One of the pioneering works in the field of POC is digital microfluidics (DMF). DMF precisely manipulates the discrete droplets of fluids of small volumes to move, mix, and split on the chip surface by electrostatic forces, without the use of integrated on-chip pumps or valves.[28] This inherent feature allows for facile integration of multi-step immunoassays and the subsequent electrochemical sensing into a single chip. The design of DMF device for electrochemical immunoassay consisted of an ITO-glass top-plate

patterned by gold working electrodes (WE) and silver counter/reference (CE/RE) electrodes, and a chromium-glass bottom-plate separated by a spacer (Fig. 4b).[29] The thyroid stimulating hormone (TSH) antigen was first captured by primary antibody (Ab1) on magnetic particles, which was further bound with HRP-conjugated antibody (Ab2–HRP) in a sandwich format. HRP catalyzed the oxidation of 3,3′,5,5′-tetramethylbenzidine (TMB), resulting in a detectable current change (Fig. 4b). This electrochemical immunoassay by DMF had the LOD of 2.4 μIU/mL, compatible with clinical applications.

3.2 AuNPs-based microfluidic electrochemical detection for nucleic acids

AuNPs-implemented microfluidic electrochemical sensors are excellent candidates for POC genetic testing, which combine both the advantages of AuNPs, *e.g.* good probes for gene recognition, and efficient amplification of electrical response, and the advantages of electrochemical sensors, *e.g.* high sensitivity, low-cost, and independence of sample turbidity.

Lee *et al.* demonstrated a silicon/glass-based microfluidic device for simultaneous on-chip PCR amplification and sequence-specific electrochemical detection.[30] The microfluidic chip consisted of a sealed reaction chamber for DNA amplification, patterned electrodes on the glass substrate for electrochemical detection of amplified product, and integrated platinum heaters for precise temperature cycling and control. Several hundred copies of DNA were successfully amplified and detected in this microfluidic system with the aid of streptavidin-labeled AuNPs. In addition to serving as carriers for hybridization of PCR product, AuNPs were used as substrates for catalytic

silver deposition to amplify the electrochemical signal. With further integration of sample pretreatment into the microfluidic chip, a portable and real-time gene analysis system might be realized.

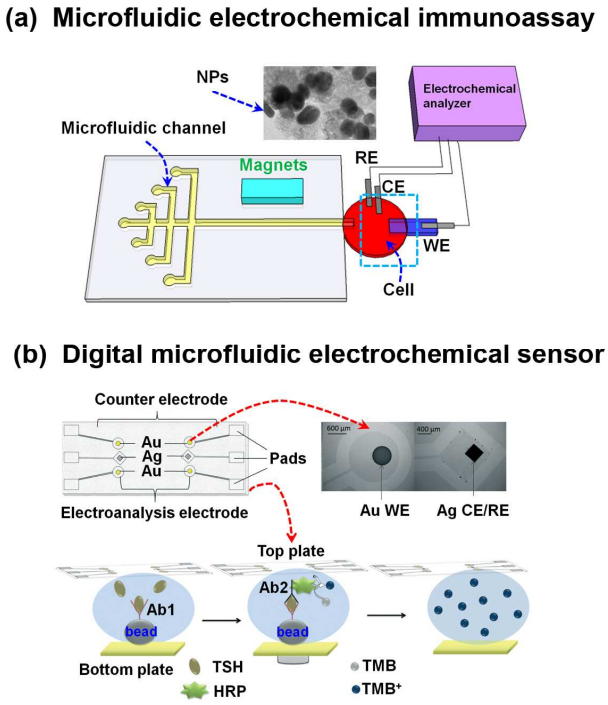

Fig. 4 (a) Experimental set-up of the microfluidic electrochemical immunoassay for detection of hemoglobin A1c (HbA1c) by using NPs composed of the gold outer shell, chitosan middle shell, and Fe_3O_4 core. Reprinted with permission from ref. [26], copyright 2011 Elsevier. (b) Digital microfluidic device for electrochemical detection of TSH antigen by a sandwich immunoassay. Reprinted with permission from ref. [29], copyright 2014 Royal Society of Chemistry.

4. AuNP-based surface plasmon resonances (SPR)

Surface plasmons are charge density oscillations at the interface of the metal and the dielectric medium. SPR is a consequence of resonance of the incident light wave with the

surface plasmon wave. For metallic nanostructures, surface plasmons are confined in the nanoscale regime, resulting in localized SPR (LSPR). Factors that determine the characteristic LSPR absorption band of nanoparticles include the species, size and shape.[31] More importantly, for a certain nanostructure like AuNPs, the surrounding environment can remarkably affect either or both of the intensity and frequency of LSPR absorption. Therefore, this boundary-sensitive effect has been exploited extensively for sensing purposes including protein and nucleic acid analysis.

The distinguishing advantage of SPR immunoassay over conventional enzyme-linked immunosorbent assay (ELISA) is that it allows for label-free detection. Qian *et al.* employed the LSPR of gold nanoshells to construct a label-free biosensor for real-time monitoring of the biomolecular interactions in diluted whole blood (Fig. 5a).[32] By modulating the dimensions of gold nanoshells on the silica core, the LSPR wavelength could be controlled in the near-infrared region (700–1300 nm), a range where optical signals could transmit though tissues with little interference. Biotin-coated gold nanoshells on the solid substrate could capture streptavidin from the blood samples, leading to the absorbance change in a concentration-dependent manner. This label-free assay could be performed without any sample purification/separation, enabling a fast and convenient way to develop biosensors for cellular analysis. In this case, 3 μg/mL streptavidin could be assayed.

Although carried out in a label-free manner, traditional SPR is not sufficiently sensitive for the detection of protein biomarkers at low abundance in clinical samples. A feasible way to enhance the sensitivity is to cooperate SPR with other signal enhancement strategies. Combining LSPR refractive index sensing with enzymatic

signal amplification, Chen *et al.* developed a plasmon-enhanced colorimetric assay with single molecule sensitivity.[33] Due to the target binding, single HRP on the individual AuNPs catalyzed a precipitation reaction to result in the wavelength shift in the LSPR. This system could improve the sensitivity of detection by a factor of up to 50 times. This approach is promising considering that HRP is widely employed as a signal amplifier in ELISA.

Single molecule detection by SPR could also be achieved by using appropriate detectors. Orrit *et al.* reported the real-time plasmonic detection of three biotin-binding proteins at a single frequency using photothermal microscopy (Fig. 5b).[34] Photothermal spectrometry was proven to be an efficient way for single molecule detection. In this case, AuNRs were prepared with a size of 31 nm × 9nm and their corresponding longitudinal SPR at 760nm, so as to match the wavelength of the heating laser (785 nm). Biotin-functionalized AuNR would capture target of interest to induce the red shift of the longitudinal SPR of the AuNR, which could be monitored by the photothermal microscopy. The high signal-to-noise ratio enabled the detection of single protein binding event, which could be used in label-free analysis of cellular proteins.

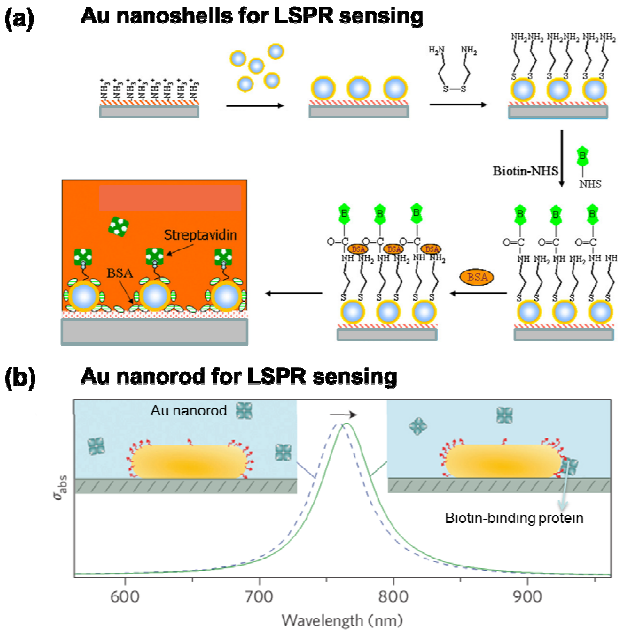

Fig. 5 AuNP-implemented SPR sensing of proteins. (a) Label-free monitoring of biomolecular interactions (biotin-streptavidin recognition) in diluted whole blood. Au nanoshells on the silica core enable LSPR sensing in the near-infrared region. Reprinted with permission from ref.[32], copyright 2008 Elsevier. (b) Plasmonic sensing of biotin-binding proteins with single molecule sensitivity using photothermal microscopy. Reprinted with permission from ref.[34], Copyright 2012 Nature Publishing Group.

4.1 AuNP-based microfluidic SPR for assaying proteins

The microfluidic platform combined with AuNPs-based detection spots has been applied for carrying out high-throughput, sensitive, and label-free SPR detection of proteins. We reported a multiplexed microfluidic immunoassay using the UV-VIS spectrophotometer as the readout on AuNPs-based LSPR substrates (Fig. 6a).[35] The customized optical bench could load and shift the microfluidic chip smoothly and precisely so that different areas in the chip were irradiated by incident light successively. The AuNPs-coated

substrate was made by the microwave plasma method to obtain a uniform distribution of the AuNPs, which were subsequently immobilized with the gp41 antigen. Multiplexed and quantitative detection of different concentrations of HIV antibody was realized in this microfluidic SPR chip by measuring the extinction spectrum of each area before and after the immobilization of anti-gp41 antibody. Compared to the standard ELISA, AuNPs-based microfluidic SPR had the similar detection limit, but this label-free method was more convenient and faster than ELISA.

Ouellet *et al.* developed an integrated microfluidic SPR array composed of 264 independent micro-chambers isolated by microvalves (Fig. 6b).[36] This device consisted of three layers: (1) The top polydimethylsiloxane (PDMS) layer containing microvalves and a micropump to control the flow of fluids beneath. (2) The middle PDMS layer with embedded microchannels for biomolecular interactions, and a parallel continuous-flow serial dilution network.[37] (3) The bottom glass substrate patterned with Au spots for SPR detection. After device assembly, streptavidin was immobilized on the Au spots, and biotinylated human α-thrombin IgG was captured by streptavidin through immunoassay. The binding process could be monitored in real-time, and the equilibrium dissociation constant was determined to be 5.0 ± 1.9 nM. A major advantage of this microfluidic, label-free SPR sensor is the ability to simultaneously interrogate hundreds of immobilization events in a single experiment.

4.2 AuNPs-based microfluidic SPR for detection of nucleic acids

While the AuNPs-based microfluidic SPR sensor has been successfully employed for real-time detection of proteins in a label-free manner, it might not be sensitive enough for

monitoring the binding kinetics of DNA of small molecular weights (< 50kDa). To expand the current microfluidic SPR system for DNA detection, Huang *et al.* fabricated the free-standing, ring-like gold nanostructures (Au nanorings) on the quartz substrate, serving as the signal amplifier in SPR detection (Fig. 6c).[38] The LSPR spectra indicated that Au nanorings had a better optical property than nanospheres and nanodisks. The assembled microfluidic SPR sensor comprised of the Au nanorings-patterned substrate was used for monitoring the hybridization between immobilized ssDNA probe and the complementary target DNA. The method could detect 100 nM of target DNA within 45 min.

Malic and co-workers reported a DMF SPR sensor based on the automated manipulation of individually addressable droplets for DNA detection.[39] To increase the SPR sensitivity, they integrated an array of periodic Au nanostructures at the sensor interface, which allowed strong optical coupling of incident light to localized surface plasmons. Using the digital SPR sensor coupled with versatile fluidic manipulation, the rapid and parallel detection of DNA hybridization was achieved within 10 min, with a sensitivity of 500 pM and sample consumption of 180 nL. This digital SPR sensor could obviate the necessity for external pumps and fluidic interconnects, which was vital for developing POC assays.

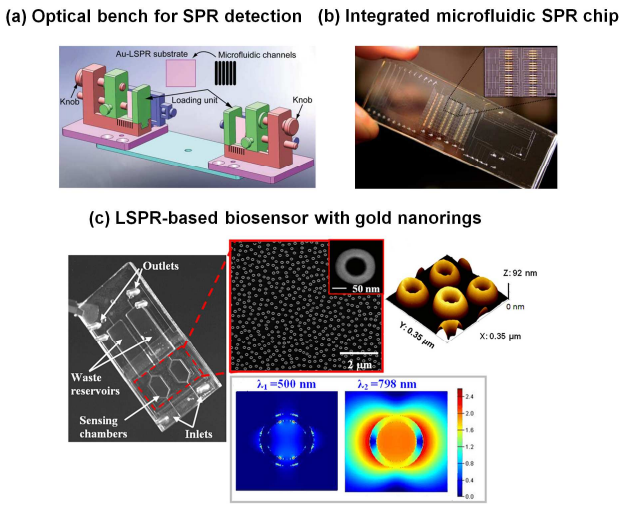

Fig. 6 (a) Schematics of a customized SPR optical bench using the UV-VIS spectrophotometer as the readout of immunoassays occurred on AuNPs-coated substrates. Reprinted with permission from ref. [35], copyright 2012 Royal Society of Chemistry. (b) An integrated microfluidic SPR device for simultaneous interrogation of hundreds of protein binding events. Reprinted with permission from ref. [36], copyright 2010 Royal Society of Chemistry. (c) The on-chip LSPR-based biosensor with gold nanorings for detection of DNA hybridization. The electric field distributions of gold nanorings at off- and on- resonant excitation wavelengths (500 nm and 798 nm) are simulated. Reprinted with permission from ref. [38], copyright 2012 American Institute of Physics.

5. AuNPs in surface-enhanced Raman scattering (SERS)

When Raman scattering occurs on the surfaces of rough metals or plasmonic nanostructures, the signal intensity can be dramatically enhanced up to 10^{14}. Though the mechanism is not fully clarified, theories including the electromagnetic theory and the chemical theory are utilized to understand the enhancement effect of SERS.[40] SERS is an important means for the analysis of proteins and nucleic acids. Owing to the remarkable

enhancement of analytical signals, SERS makes possible the spectroscopic detection of a single molecule. AuNPs and AgNPs are good candidates for further enhancing the sensitivity of SERS detection, given that their characteristic plasmon resonance frequencies coincide with the frequency of excitation light. However, for practical applications, the poor reproducibility and the wide distribution of enhancement factor still remain as challenges to be resolved. These limitations primarily originate from lack of the uniform SERS-active nanostructures including variability in particle size, shape and surface. To address this issue, Lim *et al.* presented a well-defined nanostructure (gold nano-bridged nano-gap particles, Au-NNPs) with uniform and hollow gap (~ 1 nm) for stable and reproducible SERS detection (Fig. 7a).[41] DNA-modified AuNPs were employed as the template to precisely modulate the nanostructures of Au-NNPs by DNA hybridization. Raman dyes loaded inside the nano-gap facilitated the ultrasensitive SERS detection with high stability and reproducibility. The enhancement factors were distributed within a narrow range (1.0×10^8 to 5.0×10^9), thus might be applicable for single molecule detection.

By employing Au NP-on-wire systems as a platform for SERS sensing, Kang *et al.* developed an approach for pathogen DNA detection (Fig. 7b). SERS-active nanostructures could be modulated through the DNA hybridization.[42] In the presence of target DNA, it bridged the probe DNA and reporter DNA (labeled with Raman dye) through DNA hybridization. In this way, AuNPs could assemble on the surface of Au nanowires to form a particle-on-wire structure to dramatically enhance the Raman signals. A SERS enhancement factor of 2.6×10^3 was achieved, and a DNA concentration down to 10 pM could be distinguished. A remarkable advantage of this assay was that multiple

target DNAs could be detected in only one assay if individual nanowires were assembled, which held promise for multiplex pathogen diagnostics. However, the limitation of this assay was that when it came to real clinical samples, pre-amplification of target DNA extracted from pathogenic bacteria was still required for pathogen identification.

Aside from visualized assays for nucleic acid, silver enhancement is also employed as a significant tool for SERS-based assays. Compared with AuNPs, AgNPs present better enhancement for Raman scattering. Mirkin *et al.* developed a SERS-based spectrometric approach for multiplex detection of nucleic acids.[43] In this assay, a three-component sandwich format formed upon the introduction of target DNA. Accordingly, Raman dye-labeled AuNPs were captured on the solid substrate and strong Raman signals generated after the silver enhancement. This method allowed a LOD down to 10 fM, and could differentiate single nucleotide mutation of six different viruses. However, the usage of AgNPs for real-world applications still faces challenges due to the instability as they are easily aggregated and oxidized. To circumvent this limitation, Cui *et al.* adopted Au-core/Ag-shell NPs as a stable SERS label for sandwich immunoassays.[44] Silver coating onto the Au NRs surface dramatically improved the SERS detection compared with merely the Au NRs. The high SERS enhancement factor of silver nanofilms allowed a LOD of 70 fM human IgG, which was 10^4 times lower than that of AuNRs. This strategy balances both the stability and sensitivity, and might be further improved for practical applications.

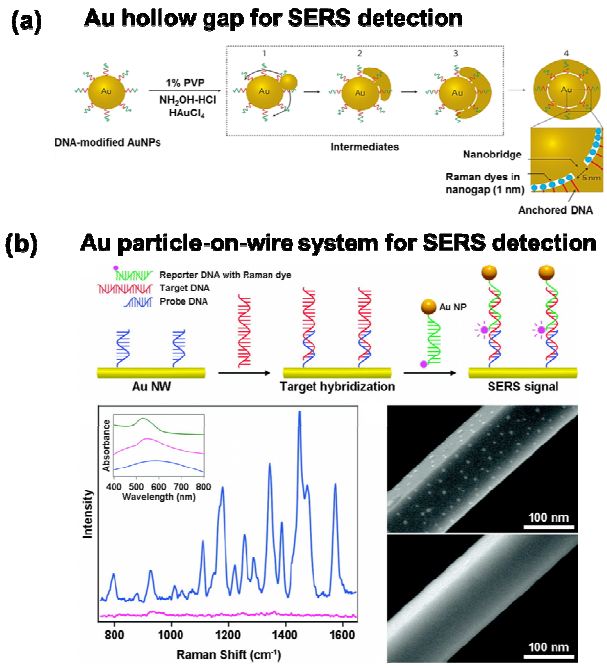

Fig. 7 AuNP-implemented SERS for DNA detection. (a) Preparation of Au-NNPs with uniform and hollow gap (~ 1 nm) via DNA hybridization for stable and reproducible SERS detection. Reprinted with permission from ref. [41], Copyright 2011 Nature Publishing Group. (b) Au particle-on-wire systems as a platform for SERS sensing. Target DNA bridges the probe DNA and reporter DNA to form a particle-on-wire structure to dramatically enhance the Raman signals. Reprinted with permission from ref. [42], Copyright 2010 American Chemical Society.

5.1 Microfluidic SERS detection of proteins using AuNPs

Microfluidic SERS-based immunoassay implemented by antibody-conjugated AuNPs is an alternative POC candidate owning to its rapid and sensitive characteristics. A recent work by Lee *et al.* presented a SERS-based microfluidic device for protein detection by using hollow gold nanospheres (HGNs) as SERS agents and gold-patterned microarray wells (Fig. 8a).[45] This chip also integrated a concentration gradient generator to obtain a

wide dynamic concentration range for immunoassay, thus obviating manual fluid handling or dilution.[37] Quantitative analysis was performed by measuring the SERS peak areas, and the LOD for rabbit AFP antigen was estimated to be 0-1 ng/mL.

Zhou *et al.* combined the modified PDMS pneumatic valve and nanopost arrays at the bottom of the fluidic microchannel to reversibly concentrate AuNPs, thus creating SERS-active sites for measuring bovine serum albumin (BSA).[46] This microfluidic SERS device could be renewed by opening the pneumatic valve and releasing the concentrated AuNPs. This method allowed a rapid protein detection within 30 min, relying on the fast aggregation of AuNPs and rapid loading of analytes. The LOD of this AuNPs-based microfluidic SERS for BSA was down to the pM level, comparable with the result by using the mass spectrometry method. The abovementioned microfluidic SERS chips could be extended for simultaneous and quantitative detection of multiple proteins, which might have a real impact on clinical POC tests.

5.2 Microfluidic SERS detection of nucleic acids using AuNPs

Microfluidic SERS devices by using AuNPs for nucleic acid detection could significantly reduce the sample consumption and shorten the reaction time, matching the goal of POC applications. Huh *et al.* reported a microfluidic SERS system to quantitatively assay Dengue Fever DNA with a LOD of 30 pM (Fig. 8b).[47] Through the enhanced mixing inside the electrokinetically active microwells, the rate of binding between the AuNPs functionalized with capture probes and the target DNA was significantly increased. The electrokinetically active microwells were also used to concentrate the hybridization product for more sensitive and rapid SERS detection. Compared to AgNPs that have been

widely used for SERS detection due to its high enhancement factor (two orders of magnitude higher than AuNPs), AuNPs posses long-term stability and high homogeneity. By adoption of electrokinetically active microwells, the sensitivity of AuNPs-based microfluidic SERS could be significantly enhanced, and even higher than AgNPs-based detection.

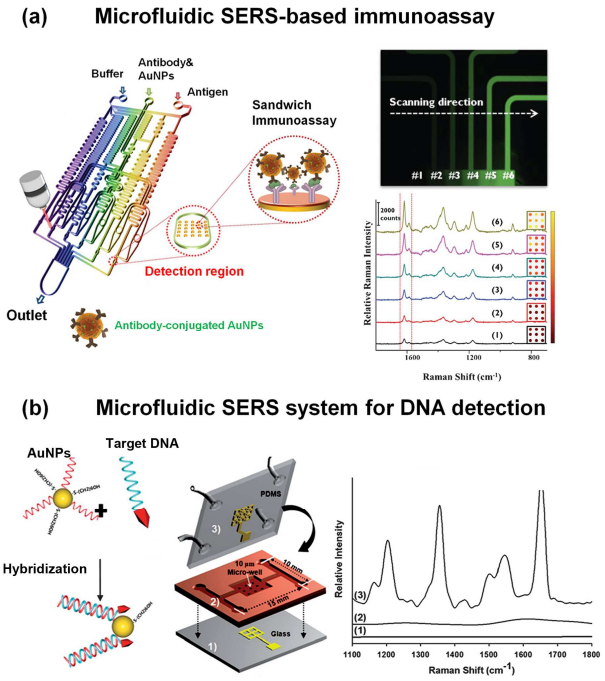

Fig. 8 (a) Schematics of a gold array-embedded gradient chip for the SERS-based immunoassay by using hollow gold nanospheres (HGNs) as SERS agents. The sandwich immunoassays are initiated on the surface of round gold wells. The microfluidic concentration gradient generator is used for serial dilution of analytes. Relative Roman intensity increases with increasing the concentration of AFP. Reprinted with permission from ref. [45], copyright 2012 Royal Society of Chemistry. (b) Schematic illustration of a microfluidic SERS system for gene detection by using functionalized AuNPs and

electrokinetically active microwells. Relative Roman intensity is enhanced after hybridization with target DNA) using the functionalized AuNPs. SERS spectra of (1) labeled AuNPs against non-specific absorption. (2) negative control, and (3) with target DNA using the functionalized AuNPs. Reprinted with permission from ref. [47], copyright 2011 Royal Society of Chemistry.

6. Portable and automated instruments for AuNP-based microfluidic chips

Although sophisticated fabrication techniques have made it possible to create miniaturized microfluidic chip with fully integrated functional structures, the operation of such chips requires bulky and complicated external equipments for fluid handling and signal readout. In particular, the use of a large number of tubes for connecting the microfluidic chip to external pumps and reservoirs may not be an acceptable form of POC diagnostics. To overcome these challenges, it would be preferable to store dried/liquid reagents inside the microfluidic device to lower the requirements for equipments.[15] Moreover, portable and automated system for sample-to-answer analysis are highly desired.

As an example of successfully commercialized POC tools, lateral strips for protein detection contain dried reagents, and the qualitative readout can be made by the naked eye in a single step. By using a strip reader or a built-in camera of the smartphone, quantitative result can be obtained (Fig. 9a). Taking advantage of the existing POC devices, for instance the personal glucose meters (PGMs), might be a feasible way to achieve portable and on-site detection of clinical biomarkers. As PGMs are initially developed for glucose sensing, the primary challenge is the signal transduction, *i.e.*, how

to establish the relationship between glucose and targets of interest in a concentration-dependent manner. Lu *et al.* exploited an aptamer-invertase system to fulfill this transduction, in which aptamer was employed for target recognition while invertase for signal transduction.[48] Analytes including metal ions, small molecules, proteins could be detected with this strategy. Since PGMs have a wide accessibility all over the world, developing assays in such a way might hold great promise for personalized medical diagnostics.

For nucleic acid and cell detection, conventional methods relying on advanced instrumentation could not be downscaled to POC formats. To address this issue, we fabricated the parallel microfluidic channels for DNA amplification, while using the low-cost optical fibers for real-time monitoring of the turbidity as a readout (Fig.9b).[49] The small-sized optical fibers could be embedded into the microfluidic chip, thus facilitating the realization of portable system for gene analysis. Another pioneering system for cell analysis is termed as Lab-on-DVD. The cell capture was performed automatically inside a multi-layered disposable polymer disc by using a modified commercial DVD drive. (Fig. 9c).[50] The DVD reader with rotational control was used for sample handling, the integrated heater was for temperature control during reaction, the photodiode array was for optical detection, and the software was for signal processing. All these components were integrated into a portable DVD system. More remarkably, the recently developed DMF allowed for programmable and automated manipulation of low volume droplets containing analytes and reagents by using a layered chip with patterned electrodes, without resorting to external pumps or fluidic interconnections. The couple of DMF and electrochemical/SPR detection could dramatically reduce the equipment size while

retaining the benefit of multiplex assays and high sensitivity.

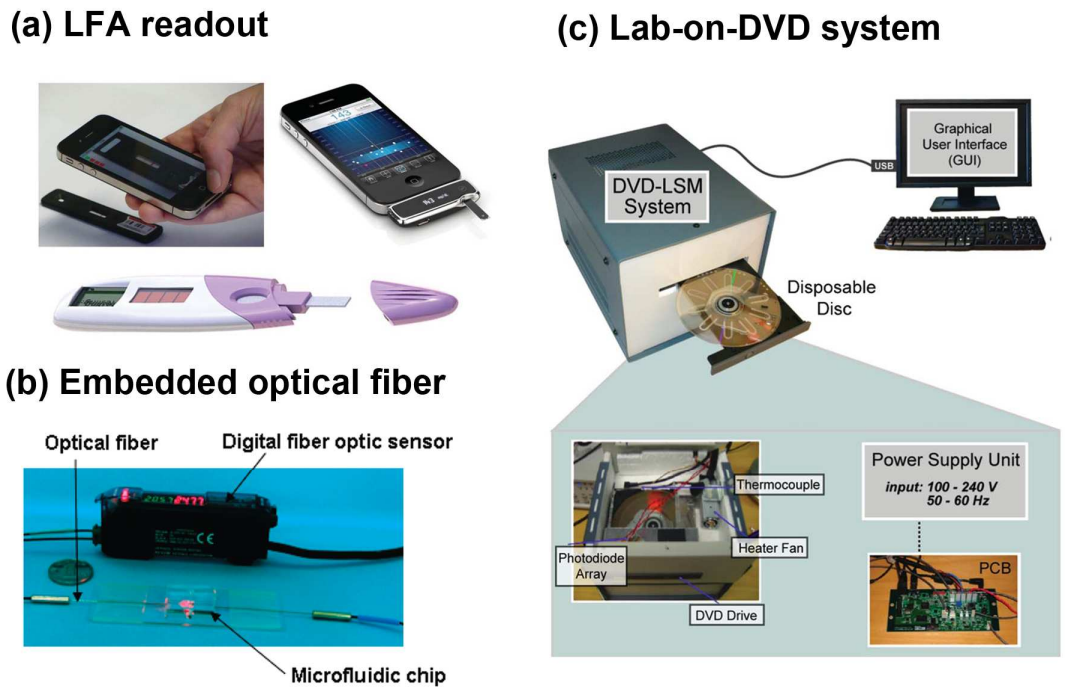

Fig. 9 Portable and automated instruments for microfluidic chips. (a) The strip reader and smartphones for LFA readout. Reprinted with permission from ref. [14], copyright 2013 Royal Society of Chemistry. (b) The embedded optical fiber with the microfluidic chip for real-time gene detection. Reprinted with permission from ref. [49], copyright 2010 American Chemical Society. (c) The integrated Lab-on-DVD system consisting of a disposable polymer disc for POC applications. Reprinted with permission from ref. [50], copyright 2013 Royal Society of Chemistry.

7. Conclusion and outlook

The development of POC diagnostic tools can have a revolutionary impact on global health. Despite of great efforts in related technologies, most systems are proof-of-concept

prototypes and require external bulk instruments. AuNPs-coupled microfluidic technologies have shown great potential to advance current diagnostic techniques in terms of increased sensitivity, throughput, integration/automation, and decreased time, cost, pretreatments. The AuNPs-implemented microfluidic may also lower the requirements of instruments. Further efforts in developing AuNPs-based microfluidic POC devices should include rational design of hybrid chips, automated manipulation of reagents, and qualitative readout by portable detection system with the ultimate goal of low-cost, high-quality assays.

Acknowledgements

We acknowledge financial support from MOST (2011CB933201, 2012AA030308, 2012AA022703 and 2013AA032204), NSFC (51105086, 91213305, 21025520, and 51073045), Chinese Academy of Sciences (XDA09030305) and Beijing Municipal Science & Technology Commission (Z131100002713024).

Table 1. A summary of biomarker sensing with different approaches

Biomarker	Disease	Approach	Sensitivity	Reference
HIV gp41	AIDS[a]	colorimetric	150 ng/mL	5
total protein	-	colorimetric	200 ng/mL	6
DNA	-	colorimetric	4.3 nM	10
DNA	-	colorimetric	1 pM	11
thrombin	coagulation	LFA[b]	2.5 nM	16
troponin I	myocardial infarction	LFA	10 pg/mL	17
hCG[c]	pregnancy	LFA	0.3 U/L	18
DNA	-	PCR[d] & LFA	0.01 fM	21
H1N1 viral RNA	influenza	PCR & LFA	4 pg/μL	22
H1N1 viral RNA	influenza	PCR & LFA	71 pg/μL	24
hemoglobin A1c	diabetes	electrochemical	0.05 μg/mL	26
PSA	prostate cancer	electrochemical	0.23 pg/mL	27
interleukin-6	immune diseases	electrochemical	0.30 pg/mL	27
TSH[e]	thyroid diseases	electrochemical	2.4 mU/L	29
DNA	-	electrochemical	0.4 fg/μL	30
streptavidin	-	SPR[f]	3 μg/mL	32
DNA	-	SERS[g]	10 fM	43
human IgG	-	SERS	70 fM	44
AFP[h]	hepatocellular carcinoma	SERS	0.625 ng/mL	45
BSA[i]	-	SERS	0.1 nM	46

[a]AIDS: acquired immune deficiency syndrome

[b]LFA: lateral flow assay

[c]hCG: human chorionic gonadotropin

[d]PCR: polymerase chain reaction

[e]TSH: thyroid stimulating hormone

[f]SPR: surface plasmon resonance

[g]SERS: surface-enhanced Raman scattering

[h]AFP: alpha fetoprotein

[i]BSA: bovine serum albumin

Table 2. A general comparison between different assays from various aspects

Approach	Colorimetry		Electrochemistry		SPR		SERS	
Format	Heterogeneous	Homogeneous (LFA)	Conventional	On-chip	Conventional	On-chip	Conventional	On-chip
Sensitivity	medium	medium	high	high	high	high	single molecule	single molecule
Accuracy	qualitative	qualitative	quantitative	quantitative	quantitative	quantitative	quantitative	quantitative
Label-free	no	no	no	no	yes	yes	no	no
Volume	mL	μL	mL	μL	mL	μL	mL	μL
Response	slow	fast	fast	fast	medium	fast	medium	fast
Readout	naked eyes	naked eyes	current/voltage	current/voltage	SPR shift	SPR shift	Raman shift	Raman shift
Cost	medium	low	high	low	high	low	high	low
Instrument	free	free	need	need	need	need	need	need
Operation	medium	simple	complicated	simple	complicated	simple	complicated	simple
Throughput	low	high	low	high	low	high	low	high
Integration	low	high	low	high	low	high	low	high

References

1. E. K. Sackmann, A. L. Fulton and D. J. Beebe, *Nature*, 2014, 507, 181-189.
2. Y. Zhang, Y. M. Guo, Y. L. Xianyu, W. W. Chen, Y. Y. Zhao and X. Y. Jiang, *Adv. Mater.*, 2013, 25, 3802-3819.
3. D. Liu, Z. Wang and X. Jiang, *Nanoscale*, 2011, 3, 1421-1433.
4. H. Jans and Q. Huo, *Chem. Soc. Rev.*, 2012, 41, 2849-2866.
5. W. Qu, Y. Liu, D. Liu, Z. Wang and X. Jiang, *Angew. Chem. Int. Edit.*, 2011, 50, 3442-3445.
6. K. Zhu, Y. Zhang, S. He, W. W. Chen, J. Z. Shen, Z. Wang and X. Y. Jiang, *Anal. Chem.*, 2012, 84, 4267-4270.
7. D. Liu, W. Chen, Y. Tian, S. He, W. Zheng, J. Sun, Z. Wang and X. Jiang, *Adv. Health. Mater.*, 2012, 1, 90-95.
8. Y. Xianyu, J. Sun, Y. Li, Y. Tian, Z. Wang and X. Jiang, *Nanoscale*, 2013, 5, 6303-6306.
9. C. S. Thaxton, D. G. Georganopoulou and C. A. Mirkin, *Clin. Chim. Acta.*, 2006, 363, 120-126.
10. H. X. Li and L. Rothberg, *Proc. Natl. Acad. Sci. U. S. A.*, 2004, 101, 14036-14039.
11. S. He, D. B. Liu, Z. Wang, K. Y. Cai and X. Y. Jiang, *Sci. China Phys. Mech.*, 2011, 54, 1757-1765.
12. F. Xia, X. L. Zuo, R. Q. Yang, Y. Xiao, D. Kang, A. Vallee-Belisle, X. Gong, J. D. Yuen, B. B. Y. Hsu, A. J. Heeger and K. W. Plaxco, *Proc. Natl. Acad. Sci. U. S. A.*, 2010, 107, 10837-10841.

13. F. B. Myers and L. P. Lee, *Lab Chip*, 2008, 8, 2015-2031.

14. A. K. Yetisen, M. S. Akram and C. R. Lowe, *Lab Chip*, 2013, 13, 2210-2251.

15. M. Hitzbleck and E. Delamarche, *Chem. Soc. Rev.*, 2013, 42, 8494-8516.

16. H. Xu, X. Mao, Q. X. Zeng, S. F. Wang, A. N. Kawde and G. D. Liu, *Anal. Chem.*, 2009, 81, 669-675.

17. D. H. Choi, S. K. Lee, Y. K. Oh, B. W. Bae, S. D. Lee, S. Kim, Y. B. Shin and M. G. Kim, *Biosens. Bioelectron.*, 2010, 25, 1999-2002.

18. E. Fu, T. Liang, J. Houghtaling, S. Ramachandran, S. A. Ramsey, B. Lutz and P. Yager, *Anal. Chem.*, 2011, 83, 7941-7946.

19. X. Y. Liu, M. Mwangi, X. J. Li, M. O'Brien and G. M. Whitesides, *Lab Chip*, 2011, 11, 2189-2196.

20. X. Mao, Y. Q. Ma, A. G. Zhang, L. R. Zhang, L. W. Zeng and G. D. Liu, *Anal. Chem.*, 2009, 81, 1660-1668.

21. P. C. Lie, J. Liu, Z. Y. Fang, B. Y. Dun and L. W. Zeng, *Chem. Commun.*, 2012, 48, 236-238.

22. N. Nagatani, K. Yamanaka, H. Ushijima, R. Koketsu, T. Sasaki, K. Ikuta, M. Saito, T. Miyahara and E. Tamiya, *Analyst*, 2012, 137, 3422-3426.

23. B. A. Rohrman and R. R. Richards-Kortum, *Lab Chip*, 2012, 12, 3082-3088.

24. Y. T. Kim, Y. Chen, J. Y. Choi, W. J. Kim, H. M. Dae, J. Jung and T. S. Seo, *Biosens. Bioelectron.*, 2012, 33, 88-94.

25. J. J. Xu, W. W. Zhao, S. P. Song, C. H. Fan and H. Y. Chen, *Chem. Soc. Rev.*, 2014, 43, 1601-1611.

26. S. P. Chen, X. D. Yu, J. J. Xu and H. Y. Chen, *Biosens. Bioelectron.*, 2011, 26,

4779-4784.

27. B. V. Chikkaveeraiah, V. Mani, V. Patel, J. S. Gutkind and J. F. Rusling, *Biosens. Bioelectron.*, 2011, 26, 4477-4483.

28. D. T. Chiu, R. M. Lorenz and G. D. M. Jeffries, *Anal. Chem.*, 2009, 81, 5111-5118.

29. M. H. Shamsi, K. Choi, A. H. Ng and A. R. Wheeler, *Lab Chip*, 2014, 14, 547-554.

30. T. M. Lee, M. C. Carles and I. M. Hsing, *Lab Chip*, 2003, 3, 100-105.

31. A. G. Brolo, *Nat. Photonics*, 2012, 6, 709-713.

32. Y. Wang, W. P. Qian, Y. Tan and S. H. Ding, *Biosens. Bioelectron.*, 2008, 23, 1166-1170.

33. S. Chen, M. Svedendahl, R. P. Van Duyne and M. Kall, *Nano. Lett.*, 2011, 11, 1826-1830.

34. P. Zijlstra, P. M. R. Paulo and M. Orrit, *Nat. Nanotechnol.*, 2012, 7, 379-382.

35. Y. Zhang, Y. Tang, Y. H. Hsieh, C. Y. Hsu, J. Xi, K. J. Lin and X. Jiang, *Lab Chip*, 2012, 12, 3012-3015.

36. E. Ouellet, C. Lausted, T. Lin, C. W. Yang, L. Hood and E. T. Lagally, *Lab Chip*, 2010, 10, 581-588.

37. X. Y. Jiang, J. M. K. Ng, A. D. Stroock, S. K. W. Dertinger and G. M. Whitesides, *J. Am. Chem. Soc.*, 2003, 125, 5294-5295.

38. C. J. Huang, J. Ye, S. Wang, T. Stakenborg and L. Lagae, *Appl. Phys. Lett.*, 2012, 100.

39. L. Malic, T. Veres and M. Tabrizian, *Biosens. Bioelectron.*, 2011, 26, 2053-2059.

40. X. M. Qian and S. M. Nie, *Chem. Soc. Rev.*, 2008, 37, 912-920.

41. D. K. Lim, K. S. Jeon, J. H. Hwang, H. Kim, S. Kwon, Y. D. Suh and J. M. Nam, *Nat. Nanotechnol.*, 2011, 6, 452-460.

42. T. Kang, S. M. Yoo, I. Yoon, S. Y. Lee and B. Kim, *Nano. Lett.*, 2010, 10, 1189-1193.

43. Y. W. C. Cao, R. C. Jin and C. A. Mirkin, *Science*, 2002, 297, 1536-1540.

44. L. Wu, Z. Y. Wang, S. F. Zong, Z. Huang, P. Y. Zhang and Y. P. Cui, *Biosens. Bioelectron.*, 2012, 38, 94-99.

45. M. Lee, K. Lee, K. H. Kim, K. W. Oh and J. Choo, *Lab Chip*, 2012, 12, 3720-3727.

46. J. H. Zhou, K. N. Ren, Y. H. Zhao, W. Dai and H. K. Wu, *Anal. Bioanal. Chem.*, 2012, 402, 1601-1609.

47. C. Y. Hsu, J. W. Huang and K. J. Lin, *Chem. Commun.*, 2011, 47, 872-874.

48. Y. Xiang and Y. Lu, *Nat. Chem.*, 2011, 3, 697-703.

49. X. E. Fang, Y. Y. Liu, J. L. Kong and X. Y. Jiang, *Anal. Chem.*, 2010, 82, 3002-3006.

50. H. Ramachandraiah, M. Amasia, J. Cole, P. Sheard, S. Pickhaver, C. Walker, V. Wirta, P. Lexow, R. Lione and A. Russom, *Lab Chip*, 2013, 13, 1578-1585.

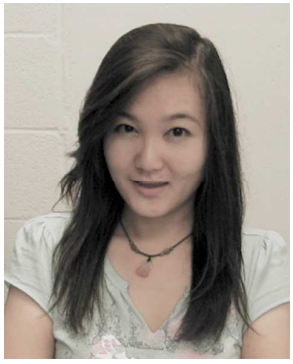

Jiashu Sun, obtained her B. S. at Beijing Institute of Technology (2006), followed by a Ph. D. (2010) from Vanderbilt University, working on microfluidics and single cell analysis. She joined the NCNST as an assistant professor in 2011 and got promoted to be an associate professor in 2013. Jiashu's research interests include microfluidics for point-of-care diagnostics, microfluidic dynamics, and nanomedicine.

Yunlei Xianyu obtained his B. S. at Huazhong University of Science and Technology (2011). He has since enrolled in a doctoral program of study at NCNST under the supervision of Prof. Xingyu Jiang. His current scientific interest is focused on nanotechnology for biomedical diagnostics.

Xingyu Jiang obtained his B. S. at the University of Chicago (1999), followed by an A. M. (2001) and a Ph. D. (2004) from Harvard University (Chemistry), working with Prof. George Whitesides. He joined the NCNST in 2005 where he has remained since. Xingyu's research interests include gold nanparticles, surface chemistry, and microfluidics.

This review focuses on assaying biomarkers using both gold nanoparticles and microfluidic devices.